16 Development of the Endbulbs of Held

Charles J. Limb and David K. Ryugo

INTRODUCTION

The cochlear nucleus of the brainstem receives direct input from the inner ear and is therefore the first synaptic station of the central auditory system. The resident neurons of the cochlear nucleus in turn give rise to all ascending pathways. Consequently, the organization between incoming auditory nerve fibers and second-order neurons plays a key role in the central processing of sound. A corollary is that abnormalities in the cochlear nucleus are likely to have downstream effects throughout the system. The cochlear nucleus contains a variety of different cell types (see Chapters 18 and 19), each of which exhibits different somatic and dendritic properties (Osen, 1969; Brawer et al., 1974), associates with a particular constellation of afferent endings (Lorente de Nó, 1981; Cant, 1982; Smith and Rhode, 1989), projects to different targets (Van Noort, 1969; Warr, 1982a; Schofield and Cant, 1996a), and expresses different response properties to sound (Pfeiffer, 1966a; Evans and Nelson, 1973; Rhode et al., 1983a; b). The particular combinations of these various properties are thought to underlie separate functions in hearing. Within the anteroventral cochlear nucleus (AVCN), myelinated auditory nerve fibers produce one or several large axosomatic endings known as endbulbs of Held (Held, 1893; Ramón y Cajal, 1909). The endbulb is one of the largest synaptic endings in the brain (Lenn and Reese, 1966), exhibits an elaborately branched appearance in adult animals (Ryugo and Fekete, 1982), expresses an estimated 500 to 2000 synaptic active zones (Ryugo et al., 1996), and contacts a population of second-order neurons called spherical bushy cells (Brawer and Morest, 1975; Cant and Morest, 1979a; Ryugo and Fekete, 1982). These features reflect a highly secure synaptic interface, consistent with the suggestion that every presynaptic discharge produces a postsynaptic spike (Pfeiffer, 1966b). The postsynaptic spherical bushy cell exhibits rapid depolarizations and repolarizations, thereby maintaining the temporal fidelity of incoming signals (Romand, 1978; Oertel, 1983; Manis and Marx, 1991). In addition, spherical bushy cells project to the superior olivary complex (Cant and Casseday, 1986) where they form a circuit implicated in the processing of interaural timing differences (Yin and Chan, 1990; Fitzpatrick et al., 1997). Thus, this component of the auditory pathway faithfully preserves the temporal changes and transients of acoustic streams necessary for the localization of sound sources in space and for the comprehension of speech (Moiseff and Konishi, 1981; Takahashi et al., 1984; Blackburn and Sachs, 1990).

The structure of endbulbs exhibits several activity-related features. Endbulb branching patterns and the ultrastructure of their synapses in cats with normal hearing have been shown to vary systematically with respect to average levels of spike discharges (Ryugo et al., 1996). The endbulbs of auditory nerve fibers having relatively low levels of spike discharges exhibit smaller swellings in their arborization and are associated with larger postsynaptic densities compared to endbulbs of relatively active fibers. Activity-related features of synaptic structure were further documented by using deafness as an extreme form of activity reduction (Ryugo et al., 1997; 1998). The endbulbs of adult congenitally deaf white cats, where auditory nerve activity is almost entirely abolished, exhibit reduced branching and hypertrophied synaptic structures when compared to hearing littermates. It

0-8493-2328-2/01/$0.00+$.50

is clear that endbulb morphology is strongly influenced by levels of activity, and most likely impacts on signal transmission from nerve to brain.

These observations have clinical implications for intervention strategies in cases of deafness. Strategies for hearing restoration have progressed from simple sound amplification to digital speech encoding and direct neuronal stimulation. The most widely used of the latter modalities is the cochlear implant, which uses an external speech processor to control an electrode array implanted within the cochlea (Marangos and Laszig, 1996; Cheng and Niparko, 1999). This array directly stimulates spiral ganglion cells, thus initiating neuronal transmission from these first-order sensory neurons to cochlear nucleus neurons of the brainstem. Thus, the physiological condition of primary neurons and their synapses is a major determinant in the success of the implant. Post-lingually deafened patients appear to benefit more from cochlear implants than pre-lingually deafened patients, and younger children benefit more than older children (Nikolopoulos et al., 1999; Waltzman et al., 1994; Gantz et al., 1994). These clinical data indicate that time windows during maturation define "critical periods" that are important factors in the normal development of the central auditory system. The endbulbs of Held may be especially relevant to the acquisition of language because speech comprehension relies on accurate temporal coding of acoustic input. It is plausible that deafness-induced abnormalities in endbulb structure and function are mostly limited to cases of congenital deafness, and that such kinds of early developmental changes are responsible for the differential effects of hearing loss in young vs. old populations. The efficacy of treatments for deafness might be improved with a better understanding of the exact nature of the changes that occur during the earliest periods of development in the auditory system.

NORMAL AND MUTANT MICE

We demonstrated in the congenitally deaf white cat that synaptic changes occur in the endbulbs of Held, where abnormal endbulb synapses appear in animals that have been deaf for 6 months or longer. One of our concerns regarding these observations, however, was whether the abnormalities of endbulb structure in congenitally deaf white cats were simply part of the genetic syndrome or whether they were due to deafness (e.g., lack of auditory nerve activity). In this regard, a different animal model was sought in order to test hypotheses developed from cat data. The mouse provides a compelling model with which to begin because of its relatively rapid development, its genetic homogeneity that limits interanimal variability, the presence of well-defined mutant strains, some with point mutations causing deafness, and the potential for single gene manipulations using transgenic techniques. A first step was to study the development of endbulbs of Held in normal-hearing mice. The next step was to compare the effects of deafness on endbulb development. The goal was to provide insight into the significance of specific time periods for proper development and the nature of activity-related features of synaptic structure. In this chapter, we report on endbulb development in normal-hearing CBA/J mice, and compare the adult endbulb morphology to that of deaf adult *shaker-2* mice (*Myo15*$^{sh2/sh2}$) and normal-hearing heterozygous littermates (*Myo15*$^{+/sh2}$).

The *shaker-2* mouse has a mutation on the MYO15 gene, causing an amino acid substitution from cysteine to tyrosine within the motor domain of the unconventional myosin 15 protein (Probst et al., 1998; see also Chapter 27). Myosin 15 appears to be involved in the maintenance of the actin organization in the hair cells of the organ of Corti and vestibular sensory epithelia. As a result of this mutation, stereocilia of homozygous mutants appear short and stubby, and the mice display phenotypic deafness and circling behavior (Deol, 1954; Probst et al., 1998). There are early pathologic alterations in the organ of Corti, but cell loss in the spiral ganglion is undetectable until after 100 days postnatal (Deol, 1954). The identified point mutation found in *shaker-2* mice has also been found in humans with DFNB3, a nonsyndromic form of recessive deafness (Wang et al., 1998). This condition emphasizes the potential of *shaker-2* mice as a model for understanding human deafness and for studying the effects of a natural form of deafness on brain development.

AUDITORY BRAIN STEM RECORDINGS (ABRS)

The bulk of the data reported in this chapter was generated from normal-hearing CBA/J mice of either sex and aged 1 day, 1 week, 2 weeks, 4 weeks, 8 to 10 weeks, and >6 months (Limb and Ryugo, 2000). The CBA/J strain of mouse was selected because it retains good hearing across most of its life span (e.g., Henry, 1983), and we needed normal baseline data with which to compare mutants. The ages of the homozygous *shaker-2* mice ($Myo15^{sh2/sh2}$) and heterozygous, hearing littermates ($Myo15^{+/sh2}$) ranged between 8 and 11 weeks. Mice were obtained from a licensed vendor (Jackson Laboratories, Bar Harbor, ME), and appeared healthy, with normal respiratory activity, normal tympanic membranes, and no evidence of external- or middle-ear infection.

Studying development in mice is not a trivial task because newborn mice are small, their peripheral auditory systems are immature (e.g., the external ear canal is closed), and they are difficult to anesthetize. Consequently, ABRs were obtained for all CBA/J mice 4 weeks of age or older. The day of birth is defined as postnatal day 1, and each successive day is numbered consecutively. All mice older than 2 weeks of age were tested for behavioral responses to free-field auditory stimuli (loud handclap from behind). CBA/J and $Myo15^{+/sh2}$ mice exhibited startle responses, but the *shaker-2* mice were unresponsive. For all mice 4 weeks of age and older, ABRs were recorded in response to clicks as a function of intensity. Mice were anesthetized using intraperitoneal injections of 3.5% chloral hydrate (0.008 mL/kg) and xylazine hydrochloride (0.006 mg/kg). ABRs were recorded with a vertex electrode and an electrode inserted behind the pinna ipsilateral to the stimulated ear. Click levels were determined in dB peak equivalent SPL (dB peSPL) referenced to 1 kHz by recording levels just inside the tip of a hollow ear bar using a calibrated microphone (Burkard, 1984). The ear bar, coupled to an electrostatic speaker (Sokolich, 1977), was then placed into the external ear canal. Clicks (n = 1000) of 100-μs duration and alternating polarity were presented monaurally in 5-dB increments, starting at 0 dB and progressing to 95 dB peSPL.

Representative ABR tracings from one 4-week-old animal and one 7-month-old animal are shown in Figure 16.1. The mean threshold for hearing in all CBA/J mice used in this study was 41.7 ± 7.1 dB peSPL, similar to previously reported values (Wenngren and Anniko, 1988; Mikaelian and Ruben, 1965; Hunter and Willott, 1987; X.Y. Zheng et al., 1999). At 4 weeks of age (n = 8), the mean threshold for hearing was 45.4 ± 9.0 dB peSPL. At 8 to 10 weeks of age (n = 6), the mean threshold was 40.2 ± 5.8 dB peSPL. At 7 months of age (n = 9), the mean threshold was 39.3 ± 5.0 dB peSPL. These differences were not statistically significant (ANOVA, $p > 0.1$), indicating that ABR thresholds are stable by 4 weeks of age and remain relatively constant for the next 6 months.

ENDBULB DEVELOPMENT

Postnatal Day 1

The newborn mouse weighed 1.33 ± 0.1 g, with a cochlear nucleus less than 0.8 mm in length. The histologic appearance of the ventral division was characterized by tightly packed cell bodies. Each cell body contained scant cytoplasm but housed a prominent nucleus. The ventral division was separated from the dorsal division by a lamina of granule cells, and the dorsal division already exhibits its characteristic layering of neuropil and cell bodies. Auditory nerve fibers were labeled by neurobiotin injections into the cochlea, and labeled fibers were observed to enter from the ventrolateral aspect, travel dorsally a short distance, and bifurcate into ascending and descending branches. At this age, individual fibers were thin (<0.5 μm in diameter) and relatively unbranched. At the rostral end of each fiber, a small terminal swelling (1 to 3 μm in diameter) could be located (Figure 16.1). Typically, the swellings appeared as rounded boutons, but the contour of the swelling

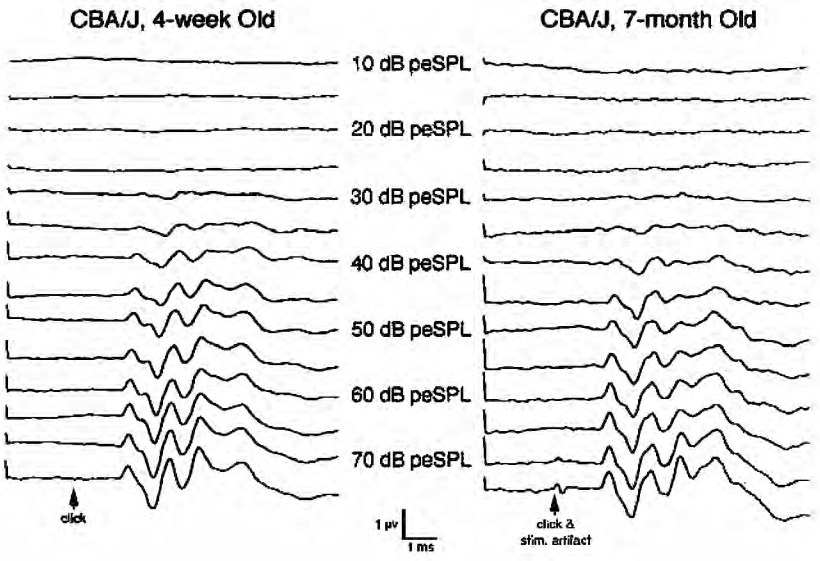

FIGURE 16.1 Representative auditory brainstem response (ABR) recordings of normal CBA/J mice, aged 4 weeks (left) and 7 months (right) in response to click stimuli. The gray arrows indicate the presentation of each click. The mean threshold of CBA/J mice (n = 23) was 41.7 ± 7.1 dB peSPL. Thresholds do not show any significant change between 4 weeks and 7 months. (Adapted from Limb and Ryugo, 2000.)

could also be elongated or triangular in shape. These terminal swellings did not resemble the mature endbulbs of Held, but we inferred their identify by virtue of their origin in the auditory nerve and their axosomatic contacts in the rostral anteroventral cochlear nucleus (AVCN).

Postnatal Week 1

During the first week, the light microscopic appearance of the swellings of auditory nerve fiber did not undergo much change. By the end of the week, the mouse weighed 3.2 ± 0.3 g, but swellings still appeared as small buds (Figure 16.2). Some of the endings were bouton-like in shape and, occasionally, two buds emanated from one fiber to form a doublet onto the same cell body. The buds themselves did not exhibit filopodia or branches.

Neurons in the rostral AVCN could not be separated into morphological groups on the basis of Nissl patterns or somatic shapes at this early age. In adults, neurons in this location are called spherical bushy cells and are described as having a round cell body, a centrally placed round nucleus surrounded by a cytoplasmic "necklace" of Nissl bodies, and a perinuclear Nissl cap (Osen, 1969; Cant and Morest, 1979a; Webster and Trune, 1982). In the neonatal mouse, the cell bodies are angular in shape and their surface is invaginated, often more than once, producing a jagged appearance. In addition, the nuclear envelope is pleated, and perinuclear Nissl caps are not observed. The mean somatic silhouette area at this age is 62.9 ± 13.8 μm^2.

Although the nuclear and cytoplasmic characteristics of cells in the rostral AVCN did not change during the first week, cell body size doubled to a mean silhouette area of 114.0 ± 14.7 μm^2. The cell outline still has frequent irregularities, but the overall impression was that they were less pronounced and that cell shape was less angular. The nuclear envelope appeared rippled, the chromatin generally dispersed, and there was no cap of perinuclear Nissl substance. In many cases, cresyl violet staining revealed the proximal portions of large dendrites.

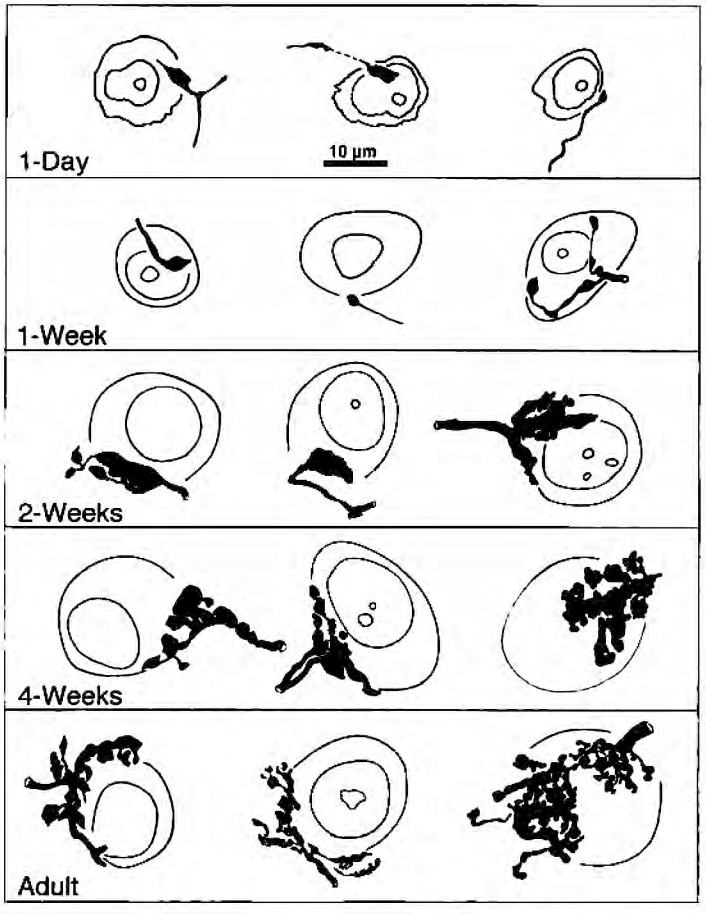

FIGURE 16.2 Representative examples of neurobiotin-labeled, axosomatic, terminal swellings in the rostral AVCN of an age-graded series of CBA/J mice, spanning from 1 day postnatal to adulthood. The endings begin as small, sometimes irregularly shaped boutons, and grow in size during the first week (Stage 0). At 2 weeks, the endings appear large, club-shaped with occasional branches (Stage 1). By 4 weeks of age, endbulbs have a central trunk that usually gives rise to two or three short branches, each of which has *en passant* swellings and bouton-like terminations (Stage 2). Adult status is reached by 9 weeks of age, and no changes in endbulb morphology can be detected out to 7 months (Stage 3). A central trunk can usually be identified that gives rise to branches that are longer and more varied in arrangement than at 4 weeks of age. The branches themselves give rise to other small branches with *en passant* swellings and complex terminations. (Adapted from Limb and Ryugo, 2000.)

Postnatal Week 2

By the end of the second postnatal week, mice weighed 5.0 ± 0.8 g and exhibited a startle response to sudden loud sounds (Mikaelian and Ruben, 1965; Ehret, 1976a; Shnerson and Pujol, 1983). The parent axon ranged from 1 to 3 µm in diameter as it ascended through the AVCN. As each axon approached one pole of the target cell, it gave rise to a large terminal swelling having a variety of shapes (Figure 16.2). The simplest endings at this age were bouton-like, but they were 10- to 15-fold larger compared to those of 1-day-old mice. A few filopodia could be seen arising from this main

swelling. In some cases, there was a coarse pattern of branches, where the parent branch gave rise to several smaller and irregular branchlets (Figure 16.2). The branchlets formed a cluster of endings that was generally confined to the same pole of the cell and did not appose much of the cell surface.

The cells of the rostral AVCN increased in mean silhouette area to 163.9 ± 18.5 μm². A perinuclear cap could be seen in stained, light microscopic preparations, revealing a defining feature of the spherical bushy cells. The contour of the cell was more regular compared to that at 1 week of age, with fewer and smaller somatic invaginations. The overall shape of the cells was oval-to-round. The nuclear envelope appeared more regular in contour and nucleoli became clearly visible.

Postnatal Week 4

At this age, CBA/J mice were approximately half their final body weight (17.4 ± 2.9 g) and terminal swellings have been replaced by endings with definite branches (Figure 16.2). These endings were identifiable as nascent endbulbs, where a central trunk (2 to 4 μm in diameter) often gave rise to more branches with *en passant* swellings and irregular terminal swellings. The main branch usually divided into two or three additional branches, each of which was nearly the same in caliber as the parent axon. The branches were separable from each other and did not extend far from the main trunk.

The cell body of the spherical bushy cell reached its adult size. The mean cross-sectional area was 204.0 ± 36.7 μm², which is significantly greater than that at 2 weeks of age ($p < 0.05$). The spherical bushy cell itself appeared similar to previous descriptions of neurons in the AVCN of cats and mice (Osen, 1969; Cant and Morest, 1979a; Webster and Trune, 1982). The cell surface lost most of its irregular contour, and now had an oval-to-round shape. The population of spherical bushy cells was generally homogeneous. The nucleus was pale and round, occupying a slightly eccentric position. Nucleoli were prominent, and a perinuclear Nissl cap had become a definable feature by light microscopic examination.

Adult Mice

Nine weeks is the mean age for initial fertile matings in mice (Crispens, 1975). At this age, the mouse weighed 30.9 ± 4.3 g and the terminal arborization of auditory nerve fibers was clearly definable as an endbulb (Figure 16.6). The main axon formed branches of approximately equal caliber, ranging from 1 to 3 μm in thickness. A central trunk with a variety of lumpy branches extended to cover up to half the somatic surface. The branches themselves gave rise to more branches with *en passant* swellings and irregular terminations, yielding an elaborate three-dimensional arrangement that encircled the cell body. Spherical bushy cells exhibited a prominent perinuclear Nissl cap and had a mean cross-sectional area of 189.8 ± 26.4 μm².

Growth continued but at a slower pace, until at least 7 months of age. On average, these old mice weighed 34.36 ± 2.9 g, and the complex pattern of endbulb arborizations persisted (Figure 16.2). The mature spherical bushy cell was characterized by a centrally located nucleus with a distinct perinuclear Nissl cap and a prominent nucleolus (Figure 16.7b). The mean cross-sectional area of spherical bushy cells in 7-month-old animals was 219.10 ± 50.2 μm².

DEAF MOUSE OBSERVATIONS

ABR Data, Shaker-2 Mice

Myo15$^{sh2/sh2}$ mice, 2 to 3 months of age, exhibited nearly constant circling behavior and were noticeably smaller (19.25 ± 0.6 g) than CBA/J mice of comparable age. At 6 months, *Myo15*$^{sh2/sh2}$ mice weighed 25.71 ± 1.3 g, approximately 75% of the weight of age-matched CBA/J mice. They exhibited no evoked potentials in response to clicks up to 95 dB peSPL (Figure 16.3), and were therefore considered deaf. Although heterozygous *Myo15*$^{+/sh2}$ littermates were also small (23.19 ± 0.6 g), they exhibited

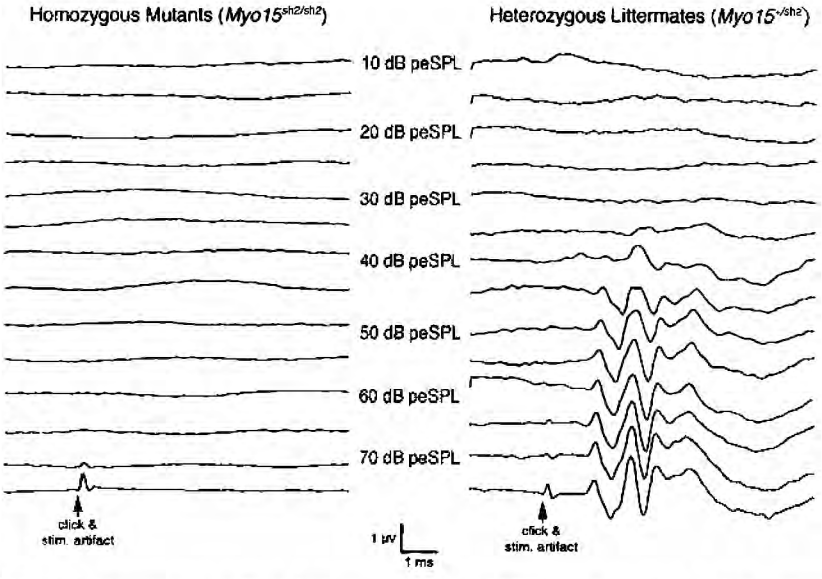

FIGURE 16.3 Representative auditory brainstem response (ABR) recordings from deaf *Myo15*$^{sh2/sh2}$ mice (left) and *Myo15*$^{+/sh2}$ littermates (right). No evoked responses were observed for *Myo15*$^{sh2/sh2}$ mice even after presentation of clicks up to 95 dB peSPL. On the right, *Myo15*$^{+/sh2}$ littermates are shown to have normal hearing in response to click stimuli, with a mean threshold of 38.5 ± 3.5 dB peSPL. The gray arrows indicate the presentation of the click stimulus. (Adapted from Limb and Ryugo, 2000.)

similar ABR thresholds (38.5 ± 3.5 dB peSPL) as those recorded in normal CBA/J mice of the same age (Figure 16.3).

Cochlear Morphology

The histologic appearance of the cochleae of CBA/J and *Myo15*$^{+/sh2}$ mice was normal, although the sample size for *Myo15*$^{+/sh2}$ was small. In contrast, the cochleae of *Myo15*$^{sh2/sh2}$ mice were distinctly abnormal. A general histopathologic description for the cochleae of *Myo15*$^{sh2/sh2}$ mice has been previously published (Deol, 1954), and our data are generally consistent with this earlier report. Briefly, the tectorial membrane is swollen in the apical turn of the cochlear duct and becomes thinner by the middle half-turn. It remained thin to the basal end. Throughout, however, the tectorial membrane failed to extend over the region of outer hair cells (OHCs). Typically, all inner hair cells were present in the apex although their intermittent absence was noted in the middle half-turn and they were mostly missing in the base. OHCs were more seriously affected. In the apex, OHCs of row 3 were often missing. Progressively more OHCs were absent throughout the rows in the middle half turn of the cochlear duct, and there were few if any OHCs in the base. The tunnel of Corti was consistently intact in the apex, but outer pillar cells were sometimes missing in the lower middle turn of the cochlear duct, and the tunnel was often difficult to discern in the base. Irrespective of the appearance of the organ of Corti, spiral ganglion cells were present throughout Rosenthal's canal for all cochleae of *Myo15*$^{sh2/sh2}$ mice. There were occasional empty spaces, 20 to 25 µm in diameter, scattered throughout Rosenthal's canal, but mostly in the basal half-turn; these spaces seemed to represent sites of ganglion cell loss. In the cochlear base, some sections exhibited up to 30% ganglion cell loss as estimated by reductions in cell density. Throughout the rest of Rosenthal's canal, however, the full complement of ganglion cells was present and appeared normal.

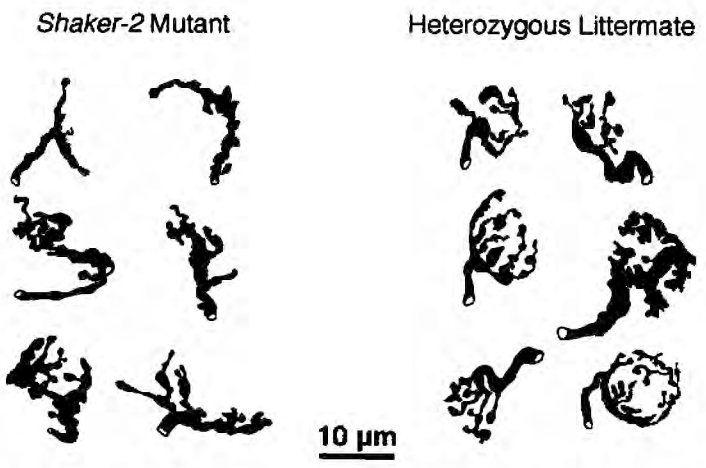

FIGURE 16.4 Drawing tube reconstructions of neurobiotin-labeled endbulbs from deaf, adult *Myo15*^{sh2} mice (left) and hearing, adult *Myo15*$^{+/sh2}$ mice (right). Endbulbs exhibit variable morphology, but overall there is a decrease in complexity of endbulb morphology in the *shaker-2* mutant mice. Many of the endbulbs of the deaf mice appear stunted in shape, without many branches or filopodia. It is particularly interesting that the endbulbs of *shaker-2* mice do not resemble those of normal mice at younger ages, suggesting that deafness does not simply arrest endbulb development. (Adapted from Limb and Ryugo, 2000.)

Endbulb Morphology

The diameter of auditory nerve fibers from 2-month-old deaf (2.88 ± 0.4 µm) and hearing (2.9 ± 0.4 µm) mice were comparable (ANOVA, $p > 0.3$). The appearance of endbulbs from normal hearing CBA/J mice of the same age. Adult hearing mice exhibited endbulbs with elaborate arborizations (Figures 16.2 and 16.4). Most striking for the deaf *Myo15*$^{sh2/sh2}$ mice was a decrease in the amount of endbulb branching (Figure 16.4). The main trunk was thick with irregular bumps, yet without interconnecting filaments or higher levels of branching. Endbulbs from deaf mice could exhibit more extensive branching and present a near normal appearance, but such occurrences were rare.

Fractal Analysis of Endbulb Complexity

Fractal geometry provides a means of quantifying the complexity of natural structures (Mandelbrot, 1982), and has been used to assess endbulb complexity (Ryugo et al., 1997). We applied the box counting technique (Fractal Dimension Calculator v1.5), in which a grid of squares having 11 different sizes is placed over the outline of an endbulb; and for each size (s), the number of squares N(s) that contain any portion of the endbulb is counted. As the size of the squares on a grid became progressively smaller, the number of intersections increased, and this increase is faster for more complicated structures. The fractal dimension D is given by the slope of the linear portion of the line when log [N(s)] is plotted against log (1/s), derived from the relationship log [N(s)] = D log (1/s). As a result, the greater the slope of the line, the greater the structural complexity. Fractal values range between 1 and 2, and each increase of 0.1 in the fractal dimension represents a doubling of structural complexity (Porter et al., 1991).

We calculated the fractal index of CBA/J endbulb silhouettes with respect to age to quantify developmental features (Figure 16.5). The mean fractal index of endbulbs progressively increases with age, beginning at 1.02 ± 0.02 in 1-day-old mice and stabilizing at 1.29 ± 0.05 at 10 weeks. The data demonstrate statistically significant changes in endbulb complexity with respect to age up to 10 weeks, but no change in complexity between the 10-week-old and the 6- to 7-month-old

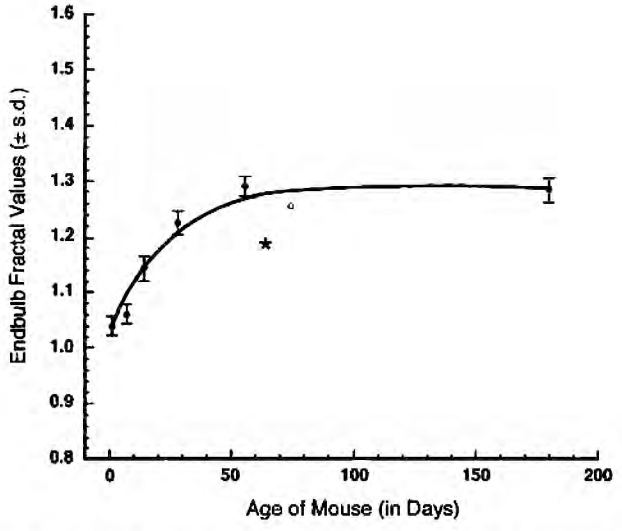

FIGURE 16.5 Graph comparing quantitative data for endbulbs of normal hearing, adult CBA/J (•) and *Myo15*$^{+/sh2}$ mice (○) to data from deaf adult *Myo15*$^{sh2/sh2}$ mice (*). This graph shows a change in fractal index with age in CBA/J mice, indicative of the increased complexity in endbulb structure. Fractal index undergoes a marked increase during the first 4 to 6 weeks of life, at which time the adult endbulb structure is reached and stabilizes throughout adulthood. Endbulb complexity is similar for hearing heterozygous *Myo15*$^{+/sh2}$ mice but seriously reduced in littermate deaf *Myo15*$^{sh2/sh2}$ mice. This graph stresses the idea that the first 2 months of life in the mouse represent a period during which significant growth, change, and structural refinement occur, and that endbulb elaboration is compromised by congenital deafness. (Adapted from Limb and Ryugo, 2000.)

mice (ANOVA, $p < 0.05$). As already stated, the fractal index (1.25 ± 0.03) of endbulbs from *Myo15*$^{+/sh2}$ mice with normal ABR thresholds was not statistically different from that of normal-hearing, adult CBA/J mice (1.29 ± 0.05). The endbulbs of deaf *shaker-2* mice, however, were less structurally complex (1.19 ± 0.04), revealing a twofold reduction in structural complexity ($p < 0.01$) and implying that endbulb structure is dependent on hearing.

Spherical Bushy Cell Size

There was a rapid, statistically significant, age-related increase in the average size of spherical bushy cells in the first month of life. Cell body size at birth was 62.9 ± 13.8 μm^2, increased to 204 ± 36.7 μm^2 at 4 weeks ($p < 0.05$), and remained constant out to 7 months of age ($p > 0.45$). The body weight of *Myo15*$^{sh2/sh2}$ and *Myo15*$^{+/sh2}$ mice was consistently less than those of age-matched CBA/J mice. Likewise, the size of their spherical bushy cells was smaller than that of adult CBA/J mice. Deaf *Myo15*$^{sh2/sh2}$ mice exhibited somatic silhouette areas of 147.68 ± 26.9 μm^2, whereas hearing *Myo15*$^{+/sh2}$ littermates exhibited a mean of 150.59 ± 32.8 μm^2. A comparison of cell body size between the three groups of mice demonstrated no difference between *Myo15*$^{sh2/sh2}$ and *Myo15*$^{+/sh2}$ mice ($p > 0.40$), but a significant difference when compared to CBA/J mice (ANOVA, $p < 0.01$). These observations suggest that cell body size is related to strain differences rather than deafness.

DISCUSSION

Endbulbs of Held represent a class of large, axosomatic synaptic endings that arise from myelinated auditory nerve fibers and terminate in the AVCN. One or several endbulbs are found on every

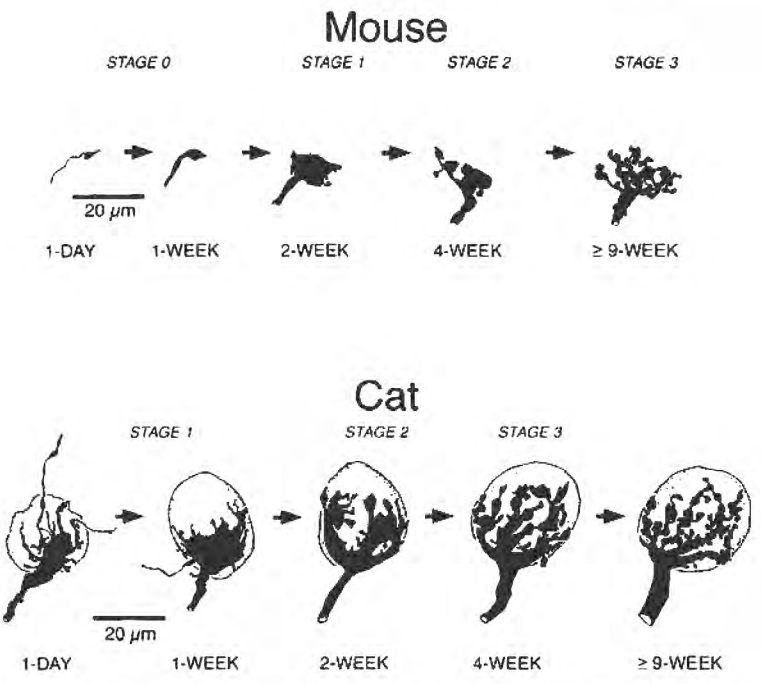

FIGURE 16.6 Developmental comparison of endbulbs of mice and cats. (Top) Schematic diagram showing developmental changes in the endbulb of Held in normal hearing CBA/J mice. The endbulb begins as a small bouton (Stage 0), grows rapidly in size to a large club-shaped ending by 2 weeks of age (Stage 1), forms definite branches by 4 weeks of age (Stage 2), and reaches its mature shape by 9 weeks of age (Stage 3). After this age, the appearance of the endbulb does not undergo significant change. (Adapted from Limb and Ryugo, 2000.) (Bottom) Schematic diagram showing the developmental appearance of endbulb of Held from cats. (Adapted from Ryugo and Fekete, 1982.) Note that the endbulbs of both species progress through essentially the same developmental stages. Reprinted by permission of Wiley-Liss, Inc., a subsidiary of John Wiley & Sons, Inc.

auditory nerve fiber, spanning the entire audible frequency range, and endbulbs are clearly identifiable throughout vertebrates (reviewed by Szpir et al., 1990). The characteristic endbulb arborization embraces the somata of spherical bushy cells, and together they form part of the circuit involved in processing of acoustic timing information. Endbulbs begin as small axosomatic swellings evident just after birth, develop gradually into larger club-shaped endings, and finally blossom into an intricate network of branches interconnected by fine filaments. This sequence of development is inferred from findings in the mouse, as well as from observations in cats (Ryugo and Fekete, 1982). Keep in mind, however, that there are differences in the duration of each developmental stage, and that the mouse auditory system seems relatively less mature at birth (Figure 16.6).

Endbulb Staging

The terminal swellings of auditory nerve fibers in the AVCN exhibit a range of appearances, but with a predominant form at each age (Figure 16.6). At the earliest ages, the presumptive endbulb appears as a simple, small bouton. During the next 2 weeks, this bud continues to enlarge, forming the classic club-shaped ending with filopodial extensions (Held, 1893; Ramón y Cajal, 1909; Lorente de Nó, 1981). This large, club-like form of the endbulb is defined as a Stage 1 endbulb in the newborn cat (Ryugo and Fekete, 1982). It appears that endbulbs of newborn mice have not yet reached this

first developmental stage, while endbulbs of newborn cats have already passed through the small bouton stage. Thus, bouton endings of the auditory nerve in the just-born mouse are defined as Stage 0 endbulbs, a stage not observed in neonatal kittens. Mice do not exhibit Stage 1 endbulbs until about 2 weeks of age. By the 4th week, the endbulb has sprouted several branches and become somewhat irregular in form. This form of the endbulb is equivalent to the Stage 2 endbulb in cats. At 9 weeks postnatal, endbulbs have become more complex in arrangement, with extensive secondary and tertiary branching that covers a large portion of the postsynaptic cell. By this age, the endbulb is considered to be adult-like and is called Stage 3. Beyond this age, endbulbs do not change in branching complexity, but become slightly finer in caliber. Thus, the endbulbs of postnatal mice begin at an earlier stage than in cats, but eventually pass through the same sequential stages of development. The qualitative descriptions of endbulbs and their staging are confirmed quantitatively by the results of fractal analysis because each stage is statistically more complex than the previous one.

Branching of Endbulbs

Development of the endbulb is likely dependent on the interaction between both pre- and postsynaptic mechanisms. The exact participants involved (whether neurotransmitters, trophic factors, action potentials, etc.) remain unidentified, but it is probable that two-way communication between endbulbs and spherical bushy cells occurs. Presynaptic activity appears to be a necessary requirement for endbulb integrity. Previous work has suggested that synapses of spherical bushy cells undergo a compensatory hypertrophy in response to sensory deprivation (Ryugo et al., 1997; 1998). What mechanisms might be responsible for such changes? Depolarization or electrical field potentials are known to influence the branching of axons and formation of lamellipodia in cultured cortical neurons (Ranmakers et al., 1998; Stewart et al., 1995; Erskine et al., 1995). Although the mechanisms underlying this branching phenomenon remain to be determined, voltage-dependent calcium channels are likely responsible for activity-dependent growth. Reduction of calcium activity has been found to block the effect of electrical current on branching (Erskine et al., 1995; Stewart et al., 1995; Graf and Cooke, 1994). Normal development of endbulbs with an intact peripheral auditory system might serve to maintain a certain minimum level of electrical activity in auditory nerve fibers, which, through a calcium-mediated process, could promote terminal branching. With deafness, however, the reduction in auditory nerve activity and presumably calcium influx might diminish terminal branching in endbulbs. Although this idea is quite speculative, the proposed mechanism is consistent with the observations in endbulb morphology associated with deafness.

Deafness and the Development of Hearing

The mouse is a useful model for study because of its homogenous genetic background, its potential for gene manipulation with transgenic techniques, and its relative immaturity at birth. The central auditory system is not functional at birth and its maturation may be dependent on that of peripheral structures. The onset of hearing in the mouse occurs around postnatal day 11, but thresholds at this age are roughly 70 dB above those of adults (Mikaelian and Ruben, 1965; Ehret, 1976a). Preyer's reflex, the acoustic startle response, is present by 9 to 14 days of age, approximately around the time that sound-evoked cochlear potentials first appear (Alford and Ruben, 1963). The organ of Corti exhibits a nearly mature appearance by the end of the second week, but continues to undergo morphologic changes until the end of the second month (Kraus and Aulbach-Kraus, 1981). Mesenchyme clears from the middle-ear space by postnatal days 14 to 16 (Mikaelian and Ruben, 1965), but the ear canal itself is not patent along its entire length until the end of the third week (unpublished observations). These findings reveal an orchestrated pattern of structural and functional development. Hearing is not only contingent on the central and peripheral maturation of auditory structures, but also on our technical and analytic abilities to detect and identify critical events.

An important distinction should be made between onset of hearing and functional hearing. By 4 weeks of age, the mice exhibited stable ABR thresholds and waveforms, despite the continued

maturation of the endbulbs of Held. It is this period between hearing readiness (around the second week) and cochlea and cochlear nucleus maturation (around the eighth week; Kraus and Aulbach-Kraus, 1981) that is crucial to the interplay between sensory input and proper development. Given that normal mice have extremely high auditory thresholds until the second postnatal week, hearing does not appear to influence early brain development. Nevertheless, the demonstration that deafness produces highly abnormal endbulbs of Held emphasizes the role of sound on development. Environmental sounds presumably enable the expression of a predetermined genetic program of development at those crucial ages.

Homozygous mutants (*Myo15*$^{sh2/sh2}$) and heterozygous littermates (*Myo15*$^{+/sh2}$) were smaller in size and body weight than CBA/J mice. These mice also had smaller spherical bushy cells. There was, however, no difference in body weight or spherical bushy cell size between these two groups of littermates. In contrast, there was a significant difference in endbulb morphology between the *Myo15*$^{sh2/sh2}$ and *Myo15*$^{+/sh2}$ mice. In the deaf *Myo15*$^{sh2/sh2}$ mouse, mature endbulbs exhibited relative structural simplicity, as evidenced by a smaller fractal index. There was no difference in endbulb complexity between *Myo15*$^{+/sh2}$ and CBA/J mice, both of which have normal hearing. These findings on endbulbs in the deaf mouse are consistent with observations in the congenitally deaf white cat (Ryugo et al., 1997; 1998) and demonstrate the effects of auditory deprivation on synaptic structure.

Endbulbs of deaf *Myo15*$^{sh2/sh2}$ mice have a similar appearance to those of congenitally deaf white cats (Ryugo et al., 1997; 1998). In deaf white cats, there is a reduction of endbulb branching complexity and a corresponding hypertrophy of postsynaptic densities (Ryugo et al., 1997). Due to the unknown genetic background of the deaf white cat, it was not known whether endbulb changes were due to the consequences of deafness or whether they were part of the constellation of abnormalities seen in the genetic syndrome. The genetic differences between deaf white cats and *Myo15*$^{sh2/sh2}$ mice in contrast to the similarities in endbulb structure, however, imply that the manifestations in endbulb abnormalities are attributable to deafness. This interpretation, while still tentative, is also the most parsimonious. Collectively, the data suggest that the endbulb synapse is responsive to both normal variations in activity (Ryugo et al., 1996) and to the pathologic absence of sound. Furthermore, the structure of these abnormal endbulbs does not resemble a state of arrested development. That is, endbulbs of normal-hearing mice and cats do not seem to pass through a stage where they resemble those of congenitally deaf animals.

The most common cause of sensorineural deafness in humans is hair cell loss within the cochlea (Kveton and Pensak, 1995). The disparate results achieved by the surgical restoration of hearing disorders, however, suggest that providing acoustic information to the brain via cochlear implantation is not by itself always sufficient to restore functionally useful hearing (Waltzman et al., 1995; Tyler and Summerfield, 1996). The endbulbs of Held, necessary for the temporal processing of sound, may be especially relevant to the acquisition of language because speech comprehension relies on accurate temporal coding of acoustic streams. Our data reveal that maturation of the endbulb and spherical bushy cell in the mouse proceeds rapidly during the first month of life and continues steadily through the second. It is plausible, then, that sound and early developmental events are responsible for the differential effects of hearing loss on young vs. old populations. The efficacy of treatments for deafness might be improved with a better understanding of the exact nature of the changes that occur at the earliest periods of auditory development. By comparing the changes seen in deafness with those seen in normal cases, we might also derive insight into the significance of particular time periods for proper development of synaptic structure.

ACKNOWLEDGMENTS

Support was provided by NIH/NIDCD research grant DC00232, NIH/NIDCD training grant DC00027, and a resident research grant from the American Academy of Otolaryngology-Head and Neck Surgery.